Available online at www.sciencedirect.com
SCIENCE DIRECT
International Journal of Heat and Mass Transfer 49 (2006) 1619–1630
International Journal of HEAT and MASS TRANSFER
www.elsevier.com/locate/ijhmt

Thermodynamic optimization of tree-shaped flow geometries

V.D. Zimparov [a,*], A.K. da Silva [b], A. Bejan [c]

[a] Department of Mechanical Engineering, Gabrovo Technical University, 4 Hadji Dimitar Str., 5300 Gabrovo, Bulgaria
[b] Department of Mechanical Engineering, University of Hawaii, Manoa, Honolulu, HI 96822, USA
[c] Department of Mechanical Engineering and Materials Science, Duke University, Box 90300, Durham, NC 27708-300, USA

Received 12 July 2005
Available online 2 February 2006

Abstract

In this paper we optimize the performance of several classes of simple flow systems consisting of T- and Y-shaped assemblies of ducts, channels and streams. In each case, the objective is to identify the geometric configuration that maximizes performance subject to several global constraints. Maximum thermodynamic performance is achieved by minimization of the entropy generated in the assemblies. The boundary conditions are fixed heat flow per unit length and uniform and constant heat flux. The flow is assumed laminar and fully developed. Every geometrical detail of the optimized structure is deduced from the constructal law. Performance evaluation criterion is proposed for evaluation and comparison of the effectiveness of different tree-shaped design heat exchangers. This criterion takes into account and compare the entropy generated in the system with heat transfer performance achieved.

Keywords: Constructal theory; Tree-shaped flow; Thermodynamic optimization; Entropy generation minimization

1. Introduction

Among the more recent methods that have become established in thermal engineering, thermodynamic optimization has the objective of improving the global performance of the system subject to specified global constraints. Thermodynamic optimization is useful as a first step, for orientation in the search of tradeoffs that govern the geometrical configuration of the system. Tree networks represent a new trend in the optimization and miniaturization of heat transfer devices [1–6], mass exchangers [7,8], chemical reactors [9], and fuel cells [10–12]. Tree-shaped architectures promise a more judicious use of the available space: higher densities of heat and mass transfer and chemical reactions, and a more uniform volumetric distribution of transport processes. The fundamental study of the optimization of tree-shaped architectures also sheds light on the common design principles of engineered and natural flow systems.

In design, and in society in general, space is at a premium. This is why the interest in performance at smaller and smaller scales is natural, and will continue. The miniaturization revolution means not only that the smallest identifiable volume element (the *elemental* system [1]) is becoming smaller, but also that larger and larger numbers of such elements must inhabit the microscopic device that they serve. The smaller the elements, and the larger their number, the greater the complexity of the structure. In design, miniaturization also means increasing complexity. Packing the system with smaller, more powerful and more numerous elemental systems is a necessary first step. The challenge is not only to find geometric arrangements to connect the currents that access the elemental systems, but to *optimize* each connection such that, ultimately, each design choice is reflected in an increase in performance at the global level. To assemble more and more elements into complex structures, and to optimize (with global objective and space constraints) each connection means to *construct*.

Improvement in the global thermodynamic performance of a system means the decrease in the irreversibility

* Corresponding author. Tel.: +359 66 223 274; fax: +359 66 801 155.
E-mail address: vdzim@tugab.bg (V.D. Zimparov).

0017-9310/$ - see front matter © 2005 Elsevier Ltd. All rights reserved.
doi:10.1016/j.ijheatmasstransfer.2005.11.016

Nomenclature

A	area (m^2)
c_p	specific heat ($J\,kg^{-1}\,K^{-1}$)
D	channel diameter (m)
f	Fanning friction factor
h	heat transfer coefficient ($W\,m^{-2}\,K^{-1}$)
k	thermal conductivity ($W\,m^{-1}\,K^{-1}$)
L	length (m)
M	dimensionless mass flow rate, $M = \dot{m}c_p/\left(\pi kNuA^{1/2}\right)$
$\dot{m}$	mass flow rate ($kg\,s^{-1}$)
N_s	entropy generation ratio, $N_s = T\dot{S}_{gen}/q$
Nu	Nusselt number, $Nu = h_iD_i/k$
n	number of pairing levels
n_0	number of central ducts
P	pressure (Pa)
q	heat flow (W)
q'	heat flow per unit length ($W\,m^{-1}$)
q''	heat flux ($W\,m^{-2}$)
$\tilde{q}'$	dimensionless heat flow per unit length, $\tilde{q}' = q'/(\pi kNuT)$
$\tilde{q}''$	dimensionless heat flux, $\tilde{q}'' = q''A^{1/2}/(\pi kNuT)$
r	radius (m)
$\dot{S}_{gen}$	entropy generation rate ($W\,K^{-1}$)
$\widetilde{S}_{gen}$	entropy generation number
T	temperature (K)
ΔT	temperature difference (K)
V	volume (m^3)
$\dot{W}$	pumping power (W), $\dot{W} = \dot{m}\Delta P/\rho$
$\widetilde{W}$	dimensionless pumping power, $\widetilde{W} = \dot{W}V^2/\left[(kNu/c_p)^2(v/\rho)A^{5/2}\right]$

Greek symbols

v	kinematic viscosity ($m^2\,s^{-1}$)
ρ	density ($kg\,m^{-3}$)
τ	$\Delta T/T$

Subscripts

i	inlet or channel rank
m	mean
n	number of construction levels
o	outlet

(or entropy generation, exergy destruction) that characterizes all the components and processes of the system. An engineering flow system owes its irreversibility to several mechanisms, most notably the flow of heat, fluid and electric current due to driving potentials, and against finite resistances. The entropy generated by each current is proportional to the product of the current times the driving potential, i.e., proportional to the resistance overcome by the current. In simple terms, the entire effort to optimize thermodynamically the greater system rests on the ability to minimize all internal flow resistances, together. Because of constraints, the resistances compete against each other.

The route to improvements in global performance is by *balancing* the reductions in the competing resistances. Thermodynamically, this amounts to spreading the entropy generation rate through the system in an optimal way, so that the total irreversibility is reduced. Optimal spreading of imperfection is achieved by properly sizing, shaping and positioning the components. In the end, the geometry structure of the system—its architecture—emerges as a result of global thermodynamic optimization.

Tree-shaped flows have been studied extensively recently [11–19]. Bejan [20], and da Silva et al. [21] proposed to use dendritic flow architecture in the conceptual design of two-stream heat exchangers. This is a new direction for the development of the heat exchanger architecture. The ultimate goal is to determine flow architectures that reach *simultaneously* two objectives: (i) minimal global fluid resistance (or pumping power), and (ii) minimal thermal resistance. When the architecture is optimized for (i), the result is a dendritic structure in which every geometric feature is uniquely determined. The corresponding thermal resistance decreases as the total mass flow rate and pumping power increase. When the objective is (ii), the optimal architecture has radial ducts, not dendrites. The corresponding fluid-flow resistance increases as the flow rate increases and the global thermal resistance decreases.

In this paper we propose a new way of approaching the geometric optimization of tree-shaped paths for fluid flow. The objective is to determine flow architectures that reach simultaneously two objectives: (i) minimal global entropy generated, and (ii) maximum heat flow density. We consider simple building block consisting of a few streams that serve as tributaries or branches in a constrained space. A larger stream with two branches (or two tributaries) forms a construct shaped as T or Y. We also show that putting together the optimized constructs it is possible to reconstruct features of the much more complicated tree structures optimized so far. Next, we show a performance evaluation criterion for evaluation of the performance of new tree-shaped flow geometries through comparison of the entropy generated in the system with the heat transfer performance achieved.

2. Boundary condition: specified heat flow per unit length

2.1. Problem formulation

In order to calculate the entropy generation, we consider an axially uniform duct of circular cross-section with a

$q' = \text{const}$ on its surface. An incompressible viscous fluid with mass flow rate $\dot{m}_i$ and inlet temperature T_i enters the channel with length L_i. The flow is laminar and fully developed (Hagen–Poiseuille). The entropy generation with a control volume of thickness $\mathrm{d}x$ along the channel is

$$\mathrm{d}\dot{S}_\text{gen} = \dot{m}\mathrm{d}s - \frac{\mathrm{d}q}{T+\Delta T}, \tag{1}$$

where

$$T(x) = T_\text{i} + 4St\frac{\Delta T}{D_i}x \tag{2}$$

is the variation of fluid temperature. In the case of incompressible fluid, $\mathrm{d}h = c_p\mathrm{d}T$, and using the thermodynamic relation $T\mathrm{d}s = \mathrm{d}h - v\mathrm{d}p$ and $\mathrm{d}q = \dot{m}\mathrm{d}h$, Eq. (1) can be written as

$$\begin{aligned}\frac{\mathrm{d}\dot{S}_\text{gen}}{\mathrm{d}x} &= \dot{m}c_p\frac{\mathrm{d}T}{\mathrm{d}x}\frac{\Delta T}{T(T+\Delta T)} + \frac{\dot{m}}{\rho T}\left(-\frac{\mathrm{d}P}{\mathrm{d}x}\right)\\ &= \dot{m}c_p\frac{\mathrm{d}T}{\mathrm{d}x}\frac{\Delta T}{T^2(1+\tau)} + \frac{\dot{m}}{\rho T}\left(-\frac{\mathrm{d}P}{\mathrm{d}x}\right).\end{aligned} \tag{3}$$

The first and second terms on the right-hand side of Eq. (3) represent the entropy generation due to heat transfer across finite temperature differences and friction, respectively. Substituting Eq. (2) into Eq. (3) and assuming that $\tau \ll 1$, Eq. (3) becomes

$$\begin{aligned}\frac{\mathrm{d}\dot{S}_\text{gen}}{\mathrm{d}x} &= \dot{m}c_p 4St\frac{\Delta T^2}{D_i}\frac{1}{\left(T_\text{i} + 4St\frac{\Delta T}{D_i}x\right)^2}\\ &\quad + \frac{\dot{m}}{\rho\left(T_\text{i} + 4St\frac{\Delta T}{D_i}x\right)}\left(-\frac{\mathrm{d}P}{\mathrm{d}x}\right).\end{aligned} \tag{4}$$

Integrating Eq. (4) along the length of the ith channel

$$\dot{S}_{\text{gen},i} = \frac{q_i\Delta T}{T_\text{i}^2}\frac{1}{\left(1+\frac{\Delta T_x^i}{T_\text{i}}\right)} + \frac{32\dot{m}_i^3 f_i L_i}{\rho^2\pi^2 T_\text{i} D_i^5}\frac{\ln\left(1+\frac{\Delta T_x^i}{T_\text{i}}\right)}{\frac{\Delta T_x^i}{T_\text{i}}}. \tag{5}$$

For simplicity, we assume that $\Delta T_x^i/T_\text{i} \ll 1$, and $T_\text{i}T_0 \cong T_\text{i}^2 \cong T_0^2$. In view of this that $q' = h_i\pi D_i\Delta T = \pi kNu\Delta T$, $q_i = q'L_i$, and $f_i = 16/Re_i = 4\pi\rho\nu D_i/\dot{m}_i$, Eq. (5) yields

$$\dot{S}_{\text{gen},i} = \frac{q'}{\pi kNuT_0^2}q'L_i + \frac{128\nu}{\rho\pi T_\text{i}}\dot{m}_i^2\frac{L_i}{D_i^4}, \tag{6}$$

where T_0 is the fluid flow temperature. For tree-shaped heat exchanger, the overall entropy generated is

$$\begin{aligned}\dot{S}_\text{gen} &= \sum_{i=0}^{n} n_i\dot{S}_{\text{gen},i}\\ &= \frac{q'}{T_0^2\pi kNu}\sum_{i=0}^{n} n_i q'L_i + \frac{128\nu}{\rho\pi T_0}\sum_{i=0}^{n} n_i\dot{m}_i^2\frac{L_i}{D_i^4},\end{aligned} \tag{7}$$

where $q = \sum_{i=0}^{n} n_i q'L_i$ is the overall heat flow. Eq. (7) can be presented in dimensionless form as follows:

$$\begin{aligned}\frac{T_0\dot{S}_\text{gen}}{q'A^{1/2}} &\equiv \widetilde{S}_\text{gen}\\ &= \frac{q'}{\pi kNuA^{1/2}T_0}\sum_{i=0}^{n} n_i L_i + \frac{128\nu}{\rho\pi q'A^{1/2}}\sum_{i=0}^{n} n_i\dot{m}_i^2\frac{L_i}{D_i^4}\end{aligned} \tag{8}$$

or

$$\begin{aligned}\frac{T_0\dot{S}_\text{gen}}{q'A^{1/2}} &\equiv \widetilde{S}_\text{gen}\\ &= \frac{\tilde{q}'}{A^{1/2}}\sum_{i=0}^{n} n_i L_i + \frac{128\nu}{\rho\pi^2\tilde{q}'T_0 kNuA^{1/2}}\sum_{i=0}^{n} n_i\dot{m}_i^2\frac{L_i}{D_i^4}.\end{aligned} \tag{9}$$

2.2. Laminar flow in a T-shaped assembly of tubes—first construct

Consider first the case of incompressible flow through the T-shaped structure, Fig. 1, for which $n = 1$, $n_i = 2^{n-i} = 2^{1-i}$, $\dot{m}_i = 2^i\dot{m}_0$, $\dot{m} = 2^n\dot{m}_0 = 2\dot{m}_0$. The flow is laminar and fully developed (Hagen–Poiseuille). The total volume occupied by the tubes is fixed,

$$V = \sum n_i\frac{\pi}{4}D_i^2L_i = \frac{\pi}{4}(2D_0^2L_0 + D_1^2L_1) = \text{const}. \tag{10}$$

Fixed is also the total space occupied by the planar structure,

$$A = (4L_0)(2L_1) = 8L_0L_1 = \text{const}. \tag{11}$$

The objective is to minimize the entropy generation number, Eq. (9). This is achieved geometrically, by selecting the proper aspect ratios that define the architecture (D_1/D_0, L_1/L_0). Since the first term in the right-hand side of Eq. (9) does not depend on D_1/D_0, the optimization of the "internal" aspect ratio D_1/D_0 gives the well know result of $D_1/D_0 = 2^{1/3}$, known as Murray's law [2]. This is another confirmation of the principle of minimum total flow resistance subject to the volume constraint. This robust result related to the aspect ratios $D_i = 2^{i/3}D_0$ will be used "a priori" in all subsequent analyses. Thus, Eq. (9) yields

$$\widetilde{S}_\text{gen} = \frac{\tilde{q}'}{A^{1/2}}\sum_{i=0}^{1} 2^{1-i}L_i + \frac{128\nu}{\rho\pi^2\tilde{q}'T_0 kNuA^{1/2}}\sum_{i=0}^{1} 2^{1-i}\dot{m}_i^2\frac{L_i}{D_i^4}, \tag{12a}$$

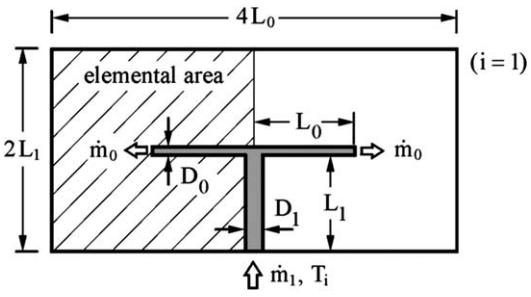

Fig. 1. T-shaped assembly of round tubes.

or

$$\widetilde{S}_{\text{gen}} = \frac{\tilde{q}'}{A^{1/2}} L_0(2+\widetilde{L}) + \frac{128 v\dot{m}^2}{\rho\pi^2\tilde{q}' T_0 kNu A^{1/2}} \frac{L_0}{2D_0^4}(1+2^{-1/3}\widetilde{L}). \tag{12b}$$

The value of D_0 is defined from the constraints:

$$A = 8L_0L_1 = 8L_0^2\widetilde{L} = \text{const}, \quad L_0 = \frac{A^{1/2}}{2^{3/2}\widetilde{L}^{1/2}}, \quad \widetilde{L} = L_1/L_0$$

and

$$V = \frac{\pi L_0 D_0^2}{2}(1+2^{-1/3}\widetilde{L}) = \text{const}.$$

Accordingly,

$$D_0^4 = \frac{4V^2}{\pi^2 L_0^2(1+2^{-1/3}\widetilde{L})^2} = \frac{32V^2}{\pi^2 A}\frac{\widetilde{L}}{(1+2^{-1/3}\widetilde{L})^2} \tag{13}$$

and Eq. (12) becomes

$$\widetilde{S}_{\text{gen}} = \frac{\tilde{q}'}{2^{3/2}}\frac{(2+\widetilde{L})}{\widetilde{L}^{1/2}} + \frac{\pi^2 vkNuA^2M^2}{2^{1/2}\rho c_p^2\tilde{q}' T_0 V^2}\frac{(1+2^{-1/3}\widetilde{L})^3}{\widetilde{L}^{3/2}} \tag{14a}$$

or

$$\widetilde{S}_{\text{gen}}\frac{2^{3/2}}{\tilde{q}'} \equiv \widetilde{S}^*_{\text{gen}} = \frac{(2+\widetilde{L})}{\widetilde{L}^{1/2}} + BM^2\frac{(1+2^{-1/3}\widetilde{L})^3}{\widetilde{L}^{3/2}}, \tag{14b}$$

where $B = \frac{2\pi^2 vkNuA^2}{\rho c_p^2 T_0 V^2 \tilde{q}'^2}$. There are two limiting cases:

(i) $M^* = BM^2 \ll 1$, when

$$\widetilde{S}^*_{\text{gen}} = \frac{(2+\widetilde{L})}{\widetilde{L}^{1/2}}, \tag{15}$$

and the minimization of $\widetilde{S}^*_{\text{gen}}(\mathrm{d}\widetilde{S}^*_{\text{gen}}/\mathrm{d}\widetilde{L} = 0)$ subject to constraints A and V yields the ratio $\widetilde{L}_{\text{opt}} = 2$.

(ii) $M^* = BM^2 \gg 1$, when

$$\widetilde{S}^*_{\text{gen}} = M^*\frac{(1+2^{-1/3}\widetilde{L})^3}{\widetilde{L}^{3/2}}, \tag{16}$$

and the minimization of $\widetilde{S}^*_{\text{gen}}$ yields the ratio $\widetilde{L}_{\text{opt}} = 2^{1/3}$. The same result was obtained in Ref. [13] from the principle of minimum global flow resistance. The variation of $\widetilde{L}_{\text{opt}}$ versus M^* can be presented as $\widetilde{L}_{\text{opt}} = 2^p$, where the variation of p versus M^* is shown in Fig. 2 (lower curve).

Fig. 3 shows one tree-shaped stream distributed over a square area. This configuration is designed from the principle of minimal global flow resistance. The numbers and flow rates are ordered as

$$n_i = 2^{n-i}, \quad \dot{m}_i = 2^i\dot{m}_0, \quad i = 0,1,\ldots,n \tag{17}$$

The lengths are obeyed the length-doubling rule by writing approximately [21]

$$L_i = 2^{i/2}L_0 \tag{18}$$

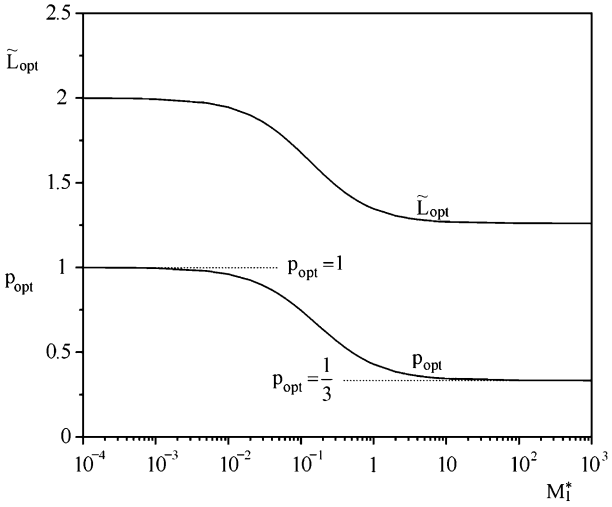

Fig. 2. The variation of $\widetilde{L}_{\text{opt}}$ and p_{opt} versus M_1^*.

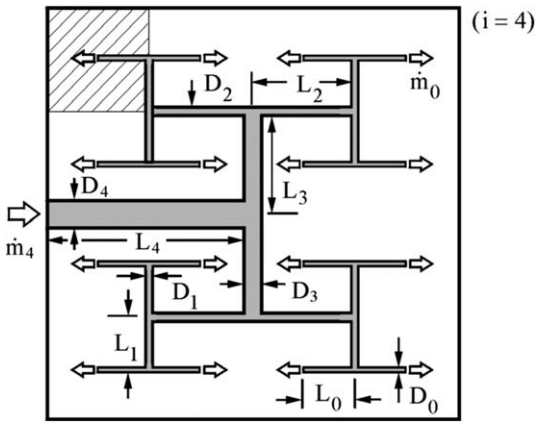

Fig. 3. Flow of tree-shaped streams distributed over a square area.

and

$$L_0 = \frac{A^{1/2}}{2^{(n+2)/2}}, \quad D_0 = \frac{2^{3/2-n/4}V^{1/2}}{\pi^{1/2}A^{1/4}S_1^{1/2}}.$$

For this case, the entropy generation number $\widetilde{S}_{\text{gen}}$, Eq. (9), becomes

$$\widetilde{S}_{\text{gen}} = \tilde{q}q' + \frac{\pi^2 vkNuA^2}{\rho c_p^2\tilde{q}' T_0 V^2}M^2\frac{S_1^3}{2^{n/2}}, \tag{19a}$$

$$\frac{\widetilde{S}_{\text{gen}}}{\tilde{q}'} = \tilde{q} + B_1M^2\frac{S_1^3}{2^{n/2}}, \tag{19b}$$

or

$$\frac{\widetilde{S}_{\text{gen}}}{\tilde{q}'} = 2^{(n-2)/2}S_2 + B_1M^2\frac{S_1^3}{2^{n/2}}, \tag{19c}$$

where

$$\frac{q}{q'A^{1/2}} \equiv \tilde{q} = 2^{(n-2)/2}S_2, \tag{19d}$$

is the overall heat flow, and

$$S_1 = \sum_{i=0}^{n} 2^{i/6} = \frac{2^{(n+1)/6} - 1}{2^{1/6} - 1},$$

$$S_2 = \sum_{i=0}^{n} 2^{-i/2} = \frac{2^{-(n+1)/2} - 1}{2^{-1/2} - 1}, \quad B_1 = \frac{\pi^2 vkNuA^2}{\rho c_p^2 \tilde{q}'^2 T_0 V^2}.$$

Eq. (19c) shows how $\widetilde{S}_{\text{gen}}$ varies with M and n, and is to be used in the case of specified M. Fig. 4 shows the variation of entropy generation number $\widetilde{S}_{\text{gen}}/\tilde{q}'$ versus complexity, n and M_1^*, where $M_1^* = B_1 M^2$. The increase of the number of branches increases the entropy generated in the system. At the same time, however, overall heat flow, Eq. (19d), increases as well. To compare the entropy generated in the system with the heat transfer performance achieved in the tree-shape design, we rearrange Eq. (19b) in the form

$$\frac{\widetilde{S}_{\text{gen}}}{\tilde{q}'\tilde{q}} = \frac{N_{\text{s}}}{\tilde{q}'} \equiv N_{\text{s}}^* = 1 + 2B_1 M^2 \frac{S_1^3}{2^n S_2}, \tag{20}$$

and define the ratio $N_{\text{s}} = \widetilde{S}_{\text{gen}}/\tilde{q}$ as a new performance evaluation criterion. The smaller N_{s} the better performance of the tree-shape flow design.

Eq. (20) presents the variation of N_{s} with M and n, and is to be used in the case of specified M. Fig. 5 (upper part) shows the variation of entropy generation ratio $N_{\text{s}}/\tilde{q}'$ versus complexity, n, and M_1^*. The entropy generation ratio does not depend on the complexity when $M_1^* \ll 1$ and takes the constant value. When M_1^* is on the order of unity or greater, the entropy generation ratio depends on the ratio $\widetilde{S} = 2^{-n} S_1^3/S_2$, Fig. 5 (lower part). Several features can be recognized from Fig. 5: (i) the entropy generation ratio has a maximum for $n \cong 5$, Fig. 5 (upper part); (ii) for values of n in the range $0 \leqslant n \leqslant 14$, the best performance gives the design with $n = 0$; (iii) whereas for $n > 14$, the greater complexity the higher returns, Fig. 5 (lower part).

In the case of fixed pumping power, $\widetilde{W} = \text{const}$, Eq. (19c) can be transformed in the form

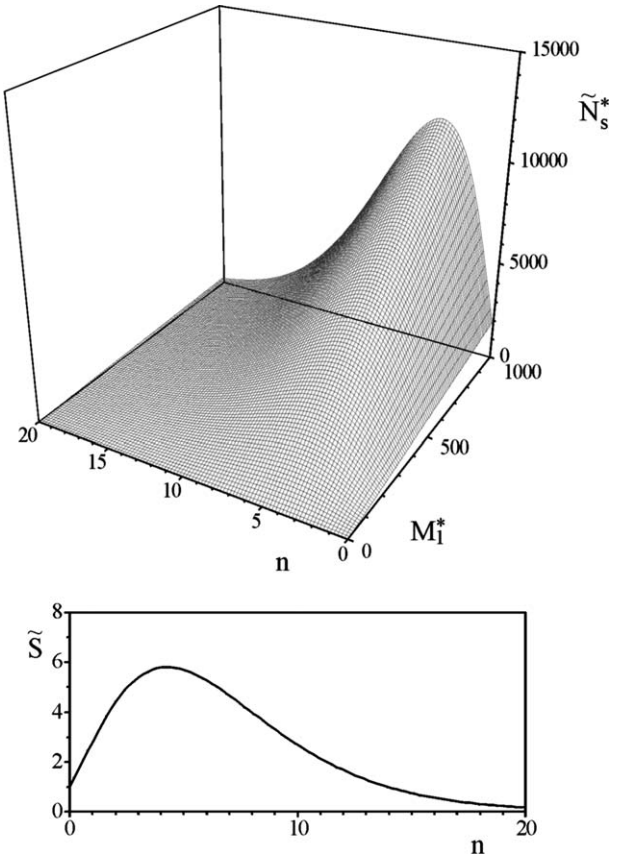

Fig. 5. Performance characteristic of tree-shaped flow distribution, Fig. 3, for fixed mass flow rate ($q' = \text{const}$).

$$\frac{\widetilde{S}_{\text{gen}}}{\tilde{q}'} = 2^{(n-2)/2} S_2 + B_1 \frac{\widetilde{W}}{\pi^3}, \tag{21}$$

where $\widetilde{W} = 2^{-n/2}\pi^3 S_1^3 M^2$ [21]. Fig. 6 shows the variation of entropy generation number, $\widetilde{S}_{\text{gen}}$, versus complexity, n, and $\widetilde{W}_1^*$, where $\widetilde{W}_1^* = B_1 \widetilde{W}/\pi^3$. As seen, the effect of complexity

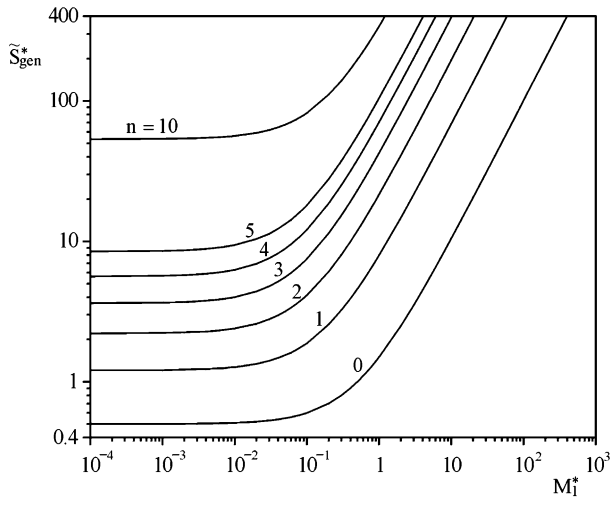

Fig. 4. The variation of entropy generation of tree-shaped flow distribution, Fig. 3, for fixed mass flow rate ($q' = \text{const}$).

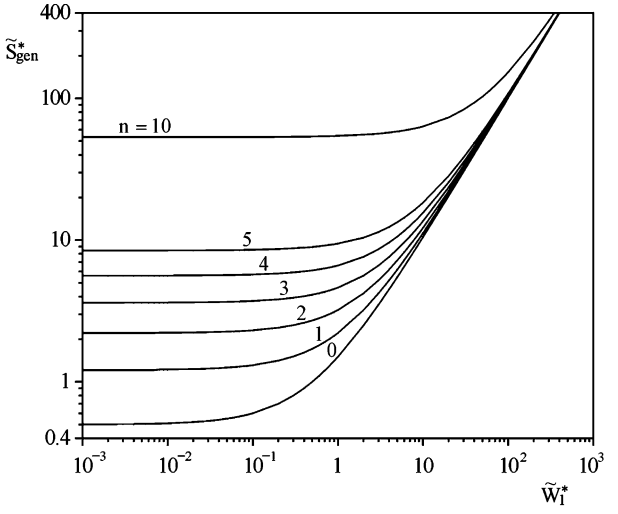

Fig. 6. The variation of entropy generation of tree-shaped flow distribution, Fig. 3, for fixed pumping power ($q' = \text{const}$).

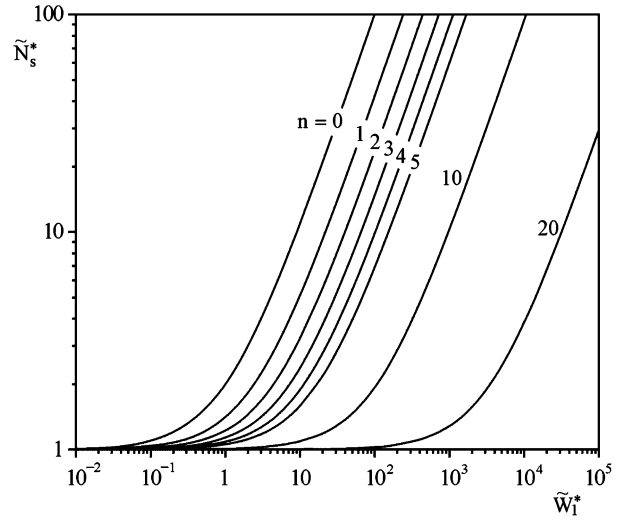

Fig. 7. Performance characteristic of tree-shaped flow distribution, Fig. 3, for fixed pumping power ($q' = \text{const}$).

on $\tilde{S}_{\text{gen}}$ almost disappears for high pumping power available. For this case, entropy generation ratio, N_s^* yields

$$\widetilde{N}_s^* = 1 + \frac{2B_1}{\pi^3}\frac{\tilde{W}}{2^{n/2}S_2}. \tag{22}$$

Fig. 7 shows the beneficial effect of complexity n on the variation of entropy generation ratio, $\widetilde{N}_s^*$, versus dimensionless pumping power W_1^*, where $W_1^* = B_1\widetilde{W}/\pi^3$. In this case, the performance of the tree-shaped heat exchanger is completely different than that in the previous case. For a fixed pumping power level, the bigger complexity the better performance of heat exchanger.

2.3. Y-shaped assembly in a circle sector

The next problem is Y-shaped construct of two L_0, and one L_1 tubes occupying the fixed area A of the circle sector of angle α, Fig. 8. The geometry of the Y-shaped construct

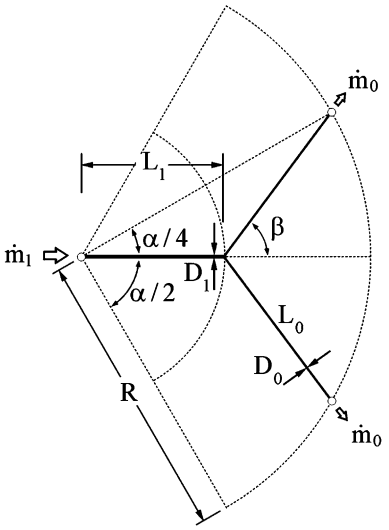

Fig. 8. Y-shaped assembly occupying a fixed area of a circle sector.

depends on the radial position of the node (i.e., the length L_1), or the angle β. Both L_0 and L_1 vary with β, when r is fixed:

$$L_0 = r\frac{\sin\left(\frac{\alpha}{4}\right)}{\sin\beta} = r\frac{\sin\left(\frac{\pi}{2n_0}\right)}{\sin\beta}, \tag{23}$$

$$L_1 = r\cos\left(\frac{\alpha}{4}\right) - r\frac{\sin\left(\frac{\alpha}{4}\right)}{\tan\beta} = r\cos\left(\frac{\pi}{2n_0}\right) - r\frac{\sin\left(\frac{\pi}{2n_0}\right)}{\tan\beta}, \tag{24}$$

$$\widetilde{L} = L_1/L_0 = \frac{\sin\beta}{\tan\left(\frac{\pi}{2n_0}\right)} - \cos\beta, \tag{25}$$

$\alpha = \frac{2\pi}{n_0}$, $A = \frac{\pi r^2}{n_0}$, and n_0 is the number of tubes leaving the centre. For this case, the expression, Eq. (12b), becomes

$$\frac{\pi^{1/2}}{\tilde{q}'}N_s \equiv N_s^* = \frac{n_0^{1/2}\sin\left(\frac{\pi}{2n_0}\right)}{\sin\beta}\left[2 + \frac{\sin\beta}{\tan\left(\frac{\pi}{2n_0}\right)} - \cos\beta\right] + B_2M^2n_0^{3/2} \times \frac{\sin^3\left(\frac{\pi}{2n_0}\right)}{\sin^3\beta}\left\{1 + 2^{-1/3}\left[\frac{\sin\beta}{\tan\left(\frac{\pi}{2n_0}\right)} - \cos\beta\right]\right\}^3, \tag{26}$$

where

$$B_2 = \frac{16\pi\nu kNuA^2}{\rho c_p^2 T_0 V^2 \tilde{q}'^2}, \quad D_0^4 = \frac{4V^2\sin^2\beta}{\pi^2 r^2\sin^2\left(\frac{\pi}{2n_0}\right)\left(1 + 2^{-1/3}\widetilde{L}\right)^2}.$$

The limiting cases are:

(i) $M_2^* = B_2M^2 \ll 0$, when

$$N_s^* = \frac{n_0^{1/2}\sin\left(\frac{\pi}{2n_0}\right)}{\sin\beta}\left[2 + \frac{\sin\beta}{\tan\left(\frac{\pi}{2n_0}\right)} - \cos\beta\right]. \tag{27}$$

The optimal angle of confluence is $\beta_{\text{opt}} = \pi/3$ rad (60°) regardless of n_0, whereas $\widetilde{L}_{\text{opt}}$ depends on n_0: $n_0 = 3$, $\widetilde{L}_{\text{opt}} = 1$; $n_0 = 5$, $\widetilde{L}_{\text{opt}} = 2.165$; $n_0 = 10$, $\widetilde{L}_{\text{opt}} = 4.967$.

(ii) $M_2^* = B_2M^2 \gg 0$, when

$$N_s^* = B_2M^2n_0^{3/2}\frac{\sin^3\left(\frac{\pi}{2n_0}\right)}{\sin^3\beta}\left\{1 + 2^{-1/3}\left[\frac{\sin\beta}{\tan\left(\frac{\pi}{2n_0}\right)} - \cos\beta\right]\right\}^3 \tag{28}$$

and the entropy minimization effort is the expression

$$R(n_0,\beta) = n_0^{3/2}\frac{\sin^3\left(\frac{\pi}{2n_0}\right)}{\sin^3\beta}\left\{1 + 2^{-1/3}\left[\frac{\sin\beta}{\tan\left(\frac{\pi}{2n_0}\right)} - \cos\beta\right]\right\}^3. \tag{29}$$

For this limiting case, the optimal angle of confluence is $\beta_{opt} = 0.654$ rad (37.47) regardless of n_0, whereas $\widetilde{L}_{opt}$ depends on n_0: $n_0 = 3$, $\widetilde{L}_{opt} = 1$; $n_0 = 5$, $\widetilde{L}_{opt} = 2.165$; $n_0 = 10$, $\widetilde{L}_{opt} = 4.967$. The same result was obtained in [18] from the principle of minimum global flow resistance. Fig. 9 shows how β_{opt} and $\widetilde{L}_{opt}$ vary with M_2^*.

Disc-shaped tree flow structure was optimized in [15] for minimum overall flow resistance. The numbers and flow rates are ordered as follows:

$$n_i = 2^{n-i} n_0, \quad \dot{m}_i = 2^{i-n} \frac{\dot{m}}{n_0}, \quad i = 0, 1, \ldots, n \tag{30}$$

The lengths are presented in dimensionless form as

$$\hat{L}_i = L_i / R, \tag{31}$$

where

$$R = \frac{A^{1/2}}{\pi^{1/2}}$$

and

$$D_0 = \frac{V^{1/2} S_3^{-1/2}}{\pi^{1/4} A^{1/4} n_n^{1/2} 2^{(n-2)/2}}.$$

For this design, the entropy generation number, Eq. (9), yields

$$\widetilde{S}_{gen} = \frac{\tilde{q}' n_0}{\pi^{1/2}} 2^n S_4 + \frac{32\pi^{1/2} vkNuA^2}{\rho c_p^2 T_0 \tilde{q}' V^2} n_0 M^2 S_3^3 \tag{32}$$

or

$$\frac{\pi^{1/2}}{\tilde{q}' n_0} \widetilde{S}_{gen} \equiv \widetilde{S}^*_{gen} = 2^n S_4 + B_3 M^2 S_3^3, \tag{33}$$

where

$$S_3 = \sum_{i=0}^{n} 2^{-i/3} \hat{L}_i, \quad S_4 = \sum_{i=0}^{n} 2^{-i} \hat{L}_i, \quad B_3 = \frac{32\pi vkNuA^2}{\rho c_p^2 T_0 \tilde{q}'^2 V^2}.$$

The overall heat flow is

$$q = 2^n n_0 q' \frac{A^{1/2}}{\pi^{1/2}} \sum_{i=0}^{n} 2^{-i} \hat{L}_i = 2^n n_0 q' \frac{A^{1/2}}{\pi^{1/2}} S_4$$

or

$$\tilde{q} \equiv \frac{\pi^{1/2} q}{q' A^{1/2} n_0} = 2^n S_4. \tag{34}$$

Eq. (33) presents the variation of $\widetilde{S}^*_{gen}$ with M and n, the case of fixed mass flow rate, $M = \text{const}$. Fig. 10 shows the variation of $\widetilde{S}_{gen}$ versus n and $M_3^* = B_3 M^2$. As seen, for small values of M_3^* the entropy generation increases gradually with the increase of complexity, whereas for high values of M_3^*, there is an optimal number of branches n_{opt} for minimal entropy generation of the system.

To compare the entropy generated in the system and heat transfer performance achieved in the tree-shape design, we rearrange Eq. (33) in the form

$$\frac{\pi^{1/2}}{\tilde{q}' n_0} \frac{\widetilde{S}_{gen}}{\tilde{q}} \equiv \tilde{N}_s^* = 1 + B_3 M^2 \frac{S_3^3}{2^n S_4}. \tag{35}$$

Eq. (35) gives the variation of $\widetilde{N}_s$ with M and n, the case of fixed mass flow rate, $M = \text{const}$. Fig. 11 shows the variation of entropy generation ratio N_s^* versus n and $M_3^* = B_3 M^2$, for $n_0 = 3$. For $M_3^* \ll 1$, the entropy generation ratio does not depend on the complexity and takes the constant value. When M_3^* is of the order of unity or greater, the entropy generation ratio gradually diminishes with the increase of complexity, and the bigger complexity the better performance of the tree-shape flow design.

In the case of fixed pumping power, $\widetilde{W} = \text{const}$, Eq. (33) yields

$$\frac{\pi^{1/2}}{\tilde{q}' n_0} \widetilde{S}_{gen} \equiv \widetilde{S}^*_{gen} = 2^n S_4 + \frac{B_3}{n_0 \pi^{3/2}} \frac{\widetilde{W}}{2^{n+3}}, \tag{36}$$

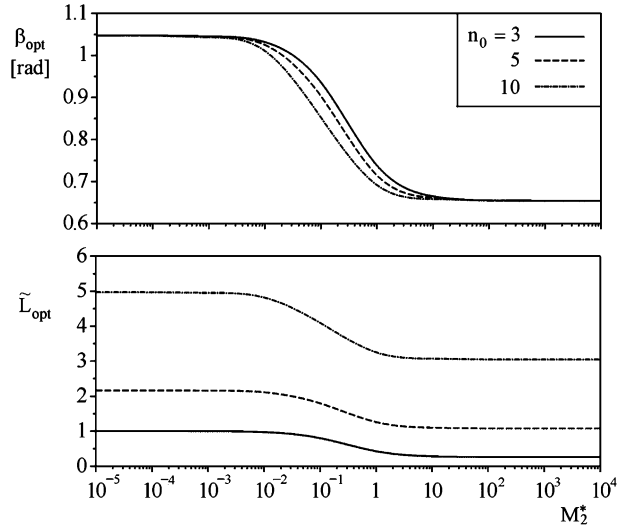

Fig. 9. The variations of β_{opt} and $\widetilde{L}_{opt}$ versus the mass flow rate ($q' = \text{const}$).

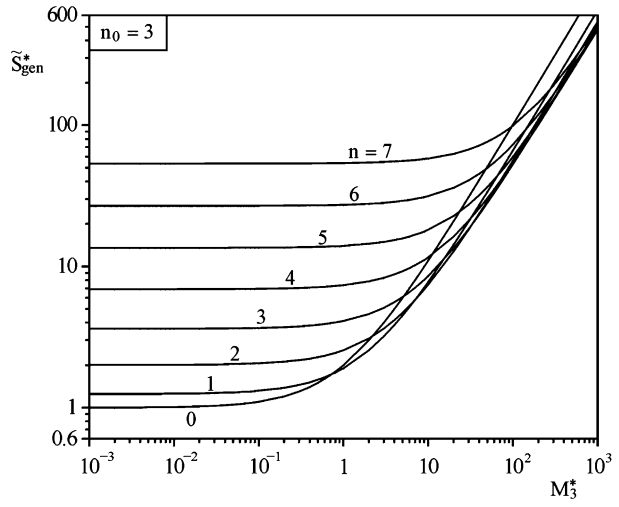

Fig. 10. The variation of entropy generation of disc-shaped tree flow distribution for fixed mass flow rate ($q' = \text{const}$).

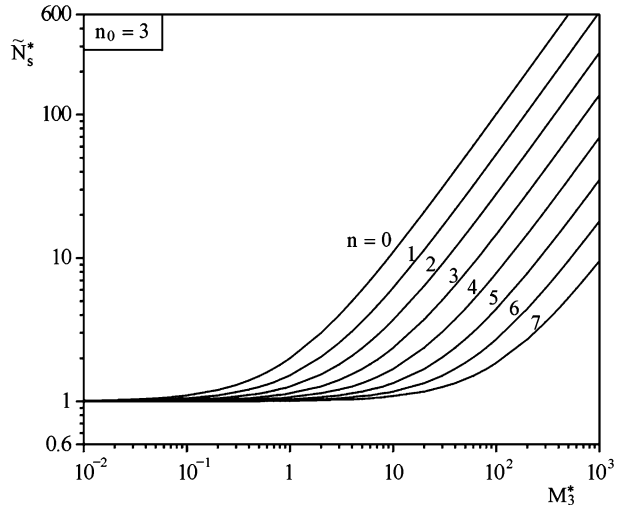

Fig. 11. Performance characteristic of disc-shaped tree flow distribution for fixed mass flow rate ($q' = \text{const}$).

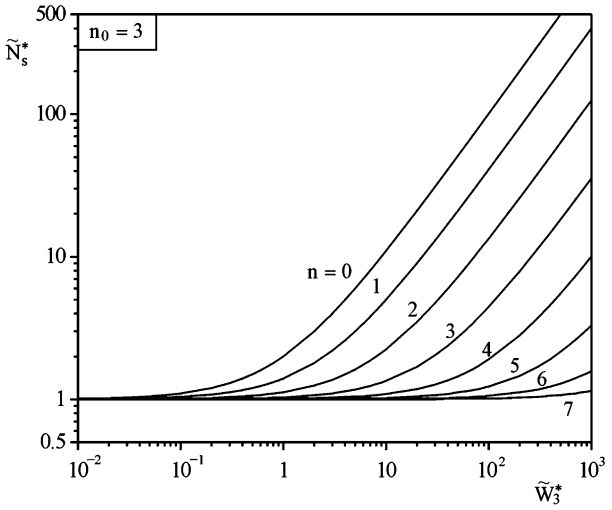

Fig. 13. Performance characteristic of disc-shaped tree flow distribution for fixed pumping power ($q' = \text{const}$).

where

$$\widetilde{W} = \pi^{3/2} 2^{n+3} n_0 S_3^3 M^2. \tag{37}$$

Fig. 12 shows the variation of entropy generation number $\widetilde{S}^*_{\text{gen}}$ versus complexity n and W^*_3, where $W^*_3 = B_3 \widetilde{W} / \left(2^3 \pi^{3/2} n_0\right)$. As seen, an envelope curve exists which gives the optimal n for any W^*_3 fixed. To compare the entropy generated in the system and heat transfer performance achieved in the tree-shape design, we rearrange Eq. (36) in the form

$$\frac{\pi^{1/2}}{\tilde{q}' n_0} \frac{\widetilde{S}_{\text{gen}}}{\tilde{q}} \equiv N^*_{\text{s}} = 1 + \frac{\widetilde{W}^*_3}{2^{2n} S_4}. \tag{38}$$

Fig. 13 shows the variation of N^*_{s} with W^*_3 and n. An remarkable trend can be recognized from the curves depicted. An defined number of channels ($n = 7$–8) exist

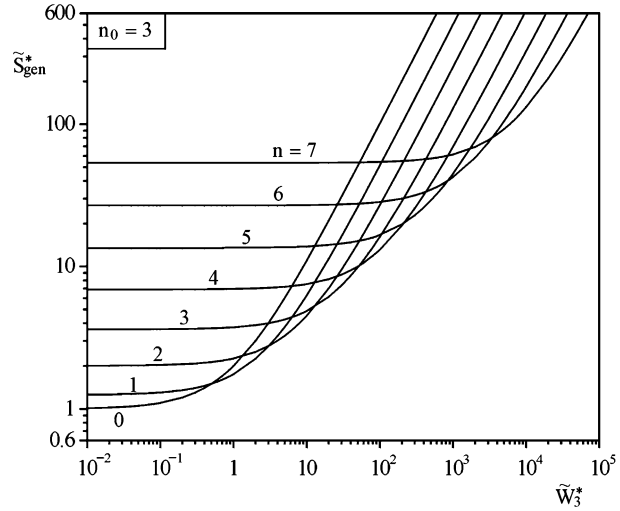

Fig. 12. The variation of entropy generation of disc-shaped tree flow distribution for fixed pumping power ($q' = \text{const}$).

that gives the maximal possible performance for this particular tree-shape flow design.

3. Boundary condition: specified heat flux

3.1. Problem formulation

In order to calculate the entropy generation, we consider an axially uniform duct of circle cross-section with a uniform heat flux, $q'' = \text{const}$, on its surface. An incompressible viscous fluid with mass flow rate $\dot{m}_i$ and inlet temperature T_{i} enters the channel with length L_i. The flow is laminar and fully developed (Hagen–Poiseuille) and the entropy generated in the ith channel is

$$\dot{S}_{\text{gen},i} = \frac{q_i \Delta T}{T_{\text{i}}^2} \frac{1}{\left(1 + \frac{\Delta T^i_x}{T_{\text{i}}}\right)} + \frac{32 \dot{m}_i^3 f_i L_i}{\rho^2 \pi^2 T_{\text{i}} D_i^5} \frac{\ln\left(1 + \frac{\Delta T^i_x}{T_{\text{i}}}\right)}{\frac{\Delta T^i_x}{T_{\text{i}}}}. \tag{5}$$

Assuming again that $\Delta T^i_x / T_{\text{i}} \ll 1$, and $T_{\text{i}} T_0 \cong T_{\text{i}}^2 \cong T_0^2$. In view of this that $q'' = h_i \Delta T = kNu \Delta T / D_i$, $q_i = q'' \pi D_i L_i$, and $f_i = 16/Re_i = 4\pi\rho\nu D_i / \dot{m}_i$, Eq. (5) yields

$$\dot{S}_{\text{gen},i} = \frac{q''}{kNu T_0^2} q_i D_i + \frac{128\nu}{\rho\pi T_{\text{i}}} \dot{m}_i^2 \frac{L_i}{D_i^4}. \tag{39}$$

For tree-shaped heat exchanger, the overall entropy generated is

$$\dot{S}_{\text{gen}} = \sum_{i=0}^{n} n_i \dot{S}_{\text{gen},i} = \frac{q''^2}{T_0^2 kNu} \sum_{i=0}^{n} n_i \pi D_i^2 L_i + \frac{128\nu}{\rho\pi T_0} \sum_{i=0}^{n} n_i \dot{m}_i^2 \frac{L_i}{D_i^4}$$

or

$$\dot{S}_{\text{gen}} = \sum_{i=0}^{n} n_i \dot{S}_{\text{gen},i} = \frac{4q''^2}{T_0^2 kNu} V + \frac{128\nu}{\rho\pi T_0} \sum_{i=0}^{n} n_i \dot{m}_i^2 \frac{L_i}{D_i^4}, \tag{40}$$

where $q = \sum_{i=0}^{n} n_i q'' \pi D_i L_i$ is the overall heat flow. Eq. (40) can be presented in dimensionless form as

$$\frac{T_0\dot{S}_{\text{gen}}}{q''A} \equiv \tilde{S}_{\text{gen}} = \frac{4q''V}{kNuT_0A} + \frac{128v}{\rho\pi Aq''}\sum_{i=0}^{n} n_i\dot{m}_i^2\frac{L_i}{D_i^4},$$

$$\widetilde{S}_{\text{gen}} = \frac{4\pi\tilde{q}''V}{A^{3/2}} + \frac{128v}{\rho\pi^2 kNuT_0\tilde{q}''A^{1/2}}\sum_{i=0}^{n} n_i\dot{m}_i^2\frac{L_i}{D_i^4},$$

or

$$\widetilde{S}_{\text{gen}} = \frac{4\pi\tilde{q}''V}{A^{3/2}}\left(1 + \frac{32vA}{\rho\pi^3 VkNuT_0\tilde{q}''^2}\sum_{i=0}^{n} n_i\dot{m}_i^2\frac{L_i}{D_i^4}\right). \tag{41}$$

3.2. Laminar flow in a T-shaped assembly of tubes—first construct

Consider again the case of incompressible flow through the T-shaped structure, Fig. 1, for which $n = 1$, $n_i = 2^{n-i} = 2^{1-i}$, $\dot{m}_i = 2^i\dot{m}_0$, $\dot{m} = 2^n\dot{m}_0 = 2\dot{m}_0$. The flow is laminar and fully developed (Hagen–Poiseuille) with the same constraints for total volume and total space occupied. The objective is to minimize the entropy generation ratio, which means to minimize the expression in the brackets of Eq. (41),

$$R = 1 + \frac{32vA}{\rho\pi^3 VkNuT_0\tilde{q}''^2}\sum_{i=0}^{n} n_i\dot{m}_i^2\frac{L_i}{D_i^4}. \tag{42}$$

For this particular case, R becomes

$$R = 1 + \frac{16vkNuA^2}{\rho c_p^2\pi VT_0\tilde{q}''^2}M^2\left(\frac{L_0}{D_0^4} + 2\frac{L_1}{D_1^4}\right)$$

or

$$R = 1 + BM^2\left(\frac{L_0}{D_0^4} + 2\frac{L_1}{D_1^4}\right), \tag{43}$$

where $B = \frac{16vkNuA^2}{\rho c_p^2\pi VT_0\tilde{q}''^2}$. There are two limiting cases:

(i) $M^* = BM^2 \ll 1$, when $R = 1$, and the entropy generation number cannot be minimized;
(ii) $M^* = BM^2 \gg 1$, when

$$R = M^*\left(\frac{L_0}{D_0^4} + 2\frac{L_1}{D_1^4}\right) \tag{44}$$

and the minimization of R yields the well known result [13] $\tilde{D}_{\text{opt}} = 2^{1/3}$ and $\tilde{L}_{\text{opt}} = 2^{1/3}$.

The entropy generation number, Eq. (41), for tree-shaped stream distributed over a square area, Fig. 2, yields

$$\widetilde{S}_{\text{gen}} = \frac{4\pi V\tilde{q}''}{A^{3/2}}\left(1 + \frac{\pi vkNuA^{7/2}M^2}{4\rho c_p^2T_0V^3\tilde{q}''^2}\frac{S_1^3}{2^{n/2}}\right)$$

or

$$\frac{\widetilde{S}_{\text{gen}}A^{3/2}}{4\pi V\tilde{q}''} = \widetilde{S}^*_{\text{gen}} = 1 + B_4M^2\frac{S_1^3}{2^{n/2}}, \tag{45}$$

where

$$B_4 = \frac{\pi vkNuA^{7/2}}{4\rho c_p^2T_0V^3\tilde{q}''^2}, \quad S_1 = \sum_{i=0}^{n}2^{i/6} = \frac{2^{(n+1)/6}-1}{2^{1/6}-1}.$$

The overall heat flow is

$$q = \sum_{i=0}^{n} n_iq''\pi D_iL_i \quad = q''A^{1/4}\pi^{1/2}V^{1/2}2^{(n+2)/4}\frac{S_5}{S_1^{1/2}},$$

or

$$\frac{qA^{3/4}}{\pi^{1/2}2^{1/2}q''AV^{1/2}} = \frac{\tilde{q}A^{3/4}}{\pi^{1/2}2^{1/2}V^{1/2}} \equiv \tilde{q}_* = \frac{2^{n/4}S_5}{S_1^{1/2}}, \tag{46}$$

where $\tilde{q} = \frac{q}{q''A}$, and $S_5 = \sum_{i=0}^{n}2^{-i/6} = \frac{2^{-(n+1)/6}-1}{2^{-1/6}-1}$.

Eq. (45) is to be used in the case of fixed mass flow, $M = \text{const}$. If the pumping power is fixed, $\widetilde{W} = \text{const}$, Eq. (45) can be transformed in the form

$$\frac{\widetilde{S}_{\text{gen}}A^{3/2}}{4\pi V\tilde{q}''} = \widetilde{S}^*_{\text{gen}} = 1 + B_4\frac{\widetilde{W}}{\pi^3}, \tag{47}$$

where $\widetilde{W} = 2^{-n/2}\pi^3S_1^3M^2$. The entropy generation ratio, $N_s = \widetilde{S}_{\text{gen}}/\tilde{q}$, yields

$$N_s = \frac{4\pi^{1/2}V^{1/2}\tilde{q}''}{A^{3/4}}\left(2^{(n+2)/4}\frac{S_1^{1/2}}{S_5} + \frac{\pi^2vkNuA^{7/2}M^2}{\rho c_p^2T_iV^3\tilde{q}''^2}\frac{S_1^{7/2}}{2^{(3n+10)/4}S_5}\right)$$

or

$$\frac{N_sA^{3/4}}{4\pi^{1/2}V^{1/2}\tilde{q}''} = \widetilde{N}^*_s = 2^{(n+2)/4}\frac{S_1^{1/2}}{S_5} + B_5M^2\frac{S_1^{7/2}}{2^{(3n+10)/4}S_5}, \tag{48}$$

where

$$B_5 = \frac{\pi^2vkNuA^{7/2}}{\rho c_p^2T_0V^3\tilde{q}''^2}, \quad S_5 = \sum_{i=0}^{n}2^{-i/6} = \frac{2^{-(n+1)/6}-1}{2^{-1/6}-1},$$

$$S_1 = \sum_{i=0}^{n}2^{i/6} = \frac{2^{(n+1)/6}-1}{2^{1/6}-1}.$$

Eq. (48) presents the case when mass flow rate is fixed, $M = \text{const}$. Fig. 14 shows the variation of entropy generation ratio $\widetilde{N}^*_s$ versus complexity, n, and $M^*_5 = B_5M^2$. In the second case, pumping power fixed, $\widetilde{W} = \text{const}$, Eq. (48) can be transformed in the form

$$\frac{N_sA^{3/4}}{4\pi^{1/2}V^{1/2}\tilde{q}''} = \widetilde{N}^*_s = 2^{(n+2)/4}\frac{S_1^{1/2}}{S_5} + \frac{B_5\widetilde{W}}{\pi^3}\frac{S_1^{1/2}}{2^{(n+10)/4}S_5}$$

or

$$\frac{N_sA^{3/4}}{4\pi^{1/2}V^{1/2}\tilde{q}''} = \widetilde{N}^*_s = \left(2^{(n+2)/4} + \frac{B_5\widetilde{W}}{\pi^32^{(n+10)/4}}\right)\frac{S_1^{1/2}}{S_5}. \tag{49}$$

Fig. 15 shows the variation of entropy generation ratio $\widetilde{N}^*_s$ versus complexity n and W^*_5.

Two very important conclusions can be derived from Figs. 12 and 14: (i) in both cases, an envelope curve exists which defines the best design configuration (complexity) according to the constraint—fixed M, or fixed $\widetilde{W}$; (ii) for

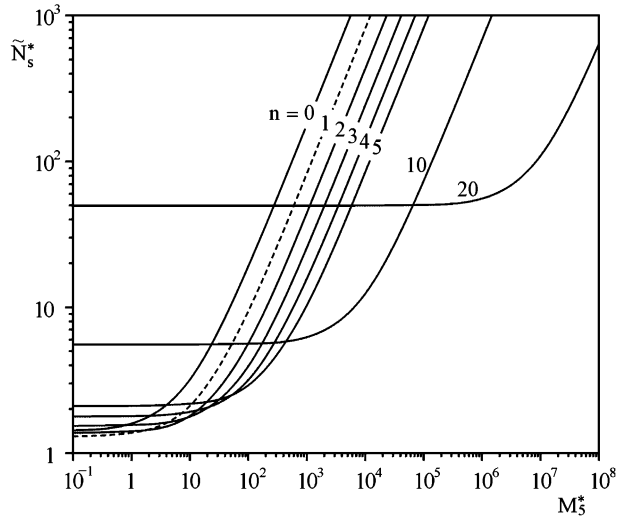

Fig. 14. Performance characteristic of tree-shaped flow distribution, Fig. 3, for fixed mass flow rate ($q'' = \text{const}$).

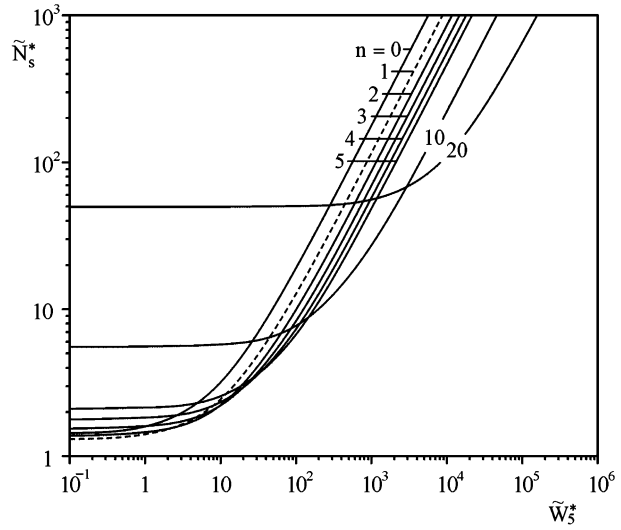

Fig. 15. Performance characteristic of tree-shaped flow distribution, Fig. 3, for fixed pumping power ($q'' = \text{const}$).

values of M_5^* or $(\widetilde{W}_5^*) < 1$, the best performance gives design with $n = 1$, not $n = 0$.

3.3. Y-shaped assembly in a disc-sector area

Consider again the case of incompressible flow through the Y-shaped construct of two L_0 tubes and one L_1 tube occupying the fixed area of the circle sector of angle α, Fig. 8. The flow is laminar and fully developed (Hagen–Poiseuille) with the same constraints for total volume and total space occupied. The objective is to minimize the entropy generation number, which means to minimize R, Eq. (38). We continue to maintain $D_i = 2^{i/3} D_0$, the principle of minimum total flow resistance subject to the volume constraint, confirmed in the previous analysis. For this case, Eq. (42) becomes

$$R = 1 + BM^2 \frac{\sin^3\left(\frac{\pi}{2n_0}\right)}{\sin^3\beta}\left\{1 + 2^{-1/3}\left[\frac{\sin\beta}{\tan\left(\frac{\pi}{2n_0}\right)} - \cos\beta\right]\right\}^3, \tag{50}$$

where $B = \frac{8\nu k N u A^{7/2}}{\rho c_p \pi^{1/2} V^3 T_0 \tilde{q}''^2}$. There are two limiting cases:

(i) $M^* = BM^2 \ll 1$, when $R = 1$, and the entropy generation number cannot be minimized;
(ii) $M^* = BM^2 \gg 1$, when

$$R = BM^2 \frac{\sin^3\left(\frac{\pi}{2n_0}\right)}{\sin^3\beta} \times \left\{1 + 2^{-1/3}\left[\frac{\sin\beta}{\tan\left(\frac{\pi}{2n_0}\right)} - \cos\beta\right]\right\}^3. \tag{51}$$

The result of the optimization process is $\beta_{\text{opt}} = 0.654$ rad (37.47). The same result was obtained in [18] from the principle of minimum global flow resistance.

For disc-shaped tree flow structure optimized in [15] from the principle of minimal global flow resistance, the entropy generation number $\widetilde{S}_{\text{gen}}$, Eq. (41), yields

$$\widetilde{S}_{\text{gen}} = \frac{4\pi\tilde{q}'' V}{A^{3/2}}\left(1 + B_6 n_0 M^2 2^n S_3^3\right)$$

or

$$\frac{A^{3/2}}{4\pi\tilde{q}'' V}\widetilde{S}_{\text{gen}} \equiv \widetilde{S}_{\text{gen}}^* = 1 + B_6 n_0 M^2 2^n S_3^3, \tag{52}$$

where $B_6 = \frac{2\nu k N u A^{7/2}}{\pi^{1/2}\rho c_p^2 T_0 V^3 \tilde{q}''^2}$, $S_3 = \sum_{i=0}^{n} 2^{-i/3}\hat{L}_i$.

Eq. (52) represents the variation of $\widetilde{S}_{\text{gen}}^*$ with M and n, the case of fixed mass flow rate ($M = \text{const}$) for particular n_0. For disc-shaped tree flow structure optimized in [15] for minimum overall flow resistance, the entropy generation ratio N_s, becomes

$$\frac{n_0^{1/2} A^{3/4}}{2\pi^{3/4} V^{1/2}}\frac{N_s}{\tilde{q}''} \equiv N_s^* = \frac{S_3^{1/2}}{2^{n/2} S_6} + B_6 n_0 M^2 \frac{2^{n/2} S_3^{7/2}}{S_6}, \tag{53}$$

where $S_3 = \sum_{i=0}^{n} 2^{-i/3}\hat{L}_i$, and $S_6 = \sum_{i=0}^{n} 2^{-2i/3}\hat{L}_i$.

Eq. (53) represents the variation of N_s^* with M and n, the case of fixed mass flow rate ($M = \text{const}$), for particular n_0. Fig. 16 shows the variation of entropy generation ratio N_s^* with complexity n and $M_6^* = n_0 B_6 M^2$, for $n_0 = 3$. Two trends can be seen: (i) for $M_6^* < 1$, the bigger the complexity the better the performance with increasing returns; (ii) for $M_6^* > 1$, the performance does not depend on the complexity and the best choice is $n = 0$.

In the case of fixed pumping power, $\tilde{W} = \text{const}$, Eq. (53) becomes

$$N_s^* = \frac{S_3^{1/2}}{2^{n/2} S_6} + \widetilde{W}_6^* \frac{S_3^{1/2}}{2^{n/2} S_6}, \tag{54}$$

where $\widetilde{W} = \pi^{3/2} 2^{n+3} n_0 S_3^3 M^2$, and $\widetilde{W}_6^* = B_6 \frac{\widetilde{W}}{2^3 \pi^{3/2}}$.

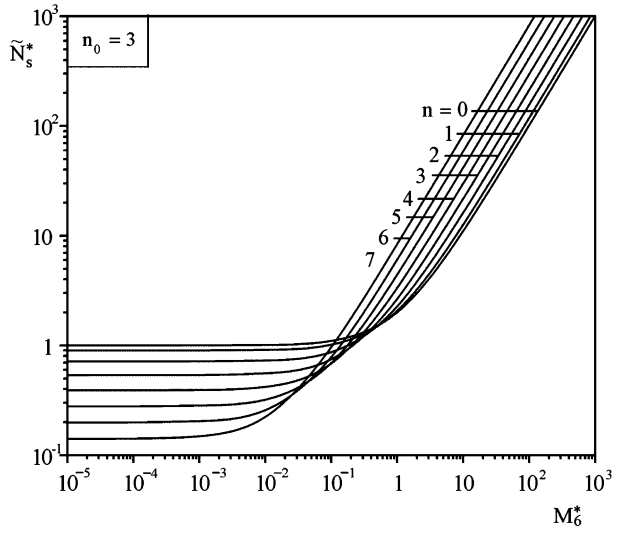

Fig. 16. Performance characteristic of disc-shaped tree flow distribution for fixed mass flow rate ($q'' = \text{const}$).

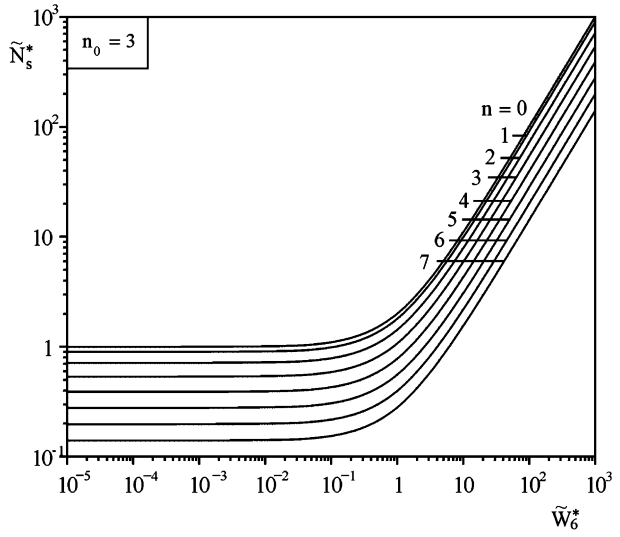

Fig. 17. Performance characteristic of disc-shaped tree flow distribution for fixed pumping power ($q'' = \text{const}$).

Fig. 17 shows the variation of entropy generation ratio N_s^*, versus complexity n, and $\widetilde{W}_6^*$. In this case, the performance does not depend on $\widetilde{W}_6^*$ and increases with the increase of the complexity with increasing returns.

4. Conclusions

In this paper we propose a new method for thermodynamic optimization to several classes of simple flow systems consisting of T- and Y-shaped assemblies of ducts, channels and streams. In each case, the objective was to identify the geometric configuration that maximized performance subject to several global constraints. The thermodynamic performance maximization is achieved by minimization of the entropy generated in the system. The boundary conditions are fixed heat flow per unit length ($q' = \text{const}$) and uniform and constant heat flux ($q'' = \text{const}$). The flow is laminar and fully developed (Hagen–Poiseuille).

The relatively simple constructs, and the various formulation of the global performance maximization problem were chosen intentionally in order to stress the most important features in the method. The maximization of the thermodynamic performance in pure fluid flow, through the minimization of the global flow resistance, is a particular case of this method. The emergence of geometric structure is a result of the consistent maximization of performance subject to constraints and every detail of the optimal flow geometry was a result of the pursuit of better global performance subject to global constraint.

Another important feature illustrated by these examples is the robustness of the optimized design for $\widetilde{D}$. The optimal ratio of the channel thickness ($\widetilde{D} = D_1/D_0$) is completely independent of the rest of the geometric parameters and global constraints. This simplifies the design of future and more complex systems, and, at the same time, insures a near-optimal performance of existing systems the structures of which may deviate from the originally intended design.

Throughout these series of examples we show that the optimized geometry has the effect of "partitioning" optimally certain features of the system. Optimal partitioning, or optimal allocation of constrained quantities is a by-product of the optimization of flow geometry. It is encountered every time global performance is maximized: optimal allocation is another way of interpreting the special optimization of the flow arrangement, i.e., *the optimal spreading of imperfection* (irreversibilities).

More fundamentally, the sequence in which the examples were presented in this paper holds an important message for future applications of the method. We started with these examples because they are the simplest, but they can serve as a base of more complicated design configurations. Moreover, the new criterion (pursuing two objectives simultaneously) is an instrument for evaluating and comparing the performance characteristics of different design configurations for the same global constraints.

Acknowledgement

V. D. Zimparov would like to express his deep gratitude to the Fulbright Commission for the financial support of his work through the Fulbright Grant 04-21-01.

References

[1] A. Bejan, Advanced Engineering Thermodynamics, second ed., Wiley, New York, 1997.
[2] A. Bejan, Shape and Structure, from Engineering to Nature, Cambridge University Press, Cambridge, UK, 2000.
[3] Y. Chen, P. Cheng, Heat transfer and pressure drop in fractal tree-like microchannel nets, Int. J. Heat Mass Transfer 45 (2002) 2643–2648.

[4] D.V. Pence, Reduced pumping power and wall temperature in microchannel heat sinks with fractal-like branching channel networks, Microscale Thermophys. Eng. 6 (2002) 319–330.
[5] A. Bejan, I. Dincer, S. Lorente, A.F. Miguel, A.H. Reis, Porous and Complex Flow Structures in Modern Technologies, Springer, New York, 2004.
[6] Z.Z. Xia, Z.-X. Li, Z.-Y. Guo, Heat conduction optimization: high conductivity constructs based on the principle of biological evolution, In: Twelfth Int. Heat Transfer Conf., Grenoble, France, 18–23 August 2002.
[7] D. Tondeur, L. Luo, U. d'Ortona, Optimisation des transferts et des des materiaux par l'approche constuctale, Entropie 30 (2000) 32–37.
[8] A. Rivera-Alvarez, A. Bejan, Constructal geometry and operation of adsorption processes, Int. J. Thermal Sci. 42 (2003) 983–994.
[9] M.-O. Coppens, Y. Cheng, C.M. van den Bleek, Controlling fluidized bed operation using a novel hierarchical gas injection system, Paper 304d, AIChE Annual Meeting, Dallas, TX, 31 October–5 November 1999.
[10] J.V.C. Vargas, A. Bejan, Thermodynamic optimization of internal structure in a fuel cell, Int. J. Energy Res. 28 (2004) 319–339.
[11] S.M. Senn, D. Poulikakos, Laminar mixing, heat transfer and pressure drop in tree-like microchannel nets and their application for thermal management in polymer electrolyte fuel cells, J. Power Sour. 130 (2004) 178–191.
[12] J.V.C. Vargas, J.C. Ordonez, A. Bejan, Constructal flow structure for a PEM fuel cell, Int. J. Heat Mass Transfer 47 (2004) 4177–4193.
[13] A. Bejan, L.A.O. Rocha, S. Lorente, Thermodynamic optimization of geometry: T- and Y-shaped constructs of fluid streams, Int. J. Thermal Sci. 30 (2000) 949–960.
[14] A. Bejan, M.R. Errera, Convective trees of fluid channels for volumetric cooling, Int. J. Heat Mass Transfer 43 (2000) 3105–3118.
[15] S. Lorente, W. Wechsatol, A. Bejan, Tree-shaped flow structures designed by minimizing path lengths, Int. J. Heat Mass Transfer 45 (2002) 3299–3312.
[16] W. Wechsatol, S. Lorente, A. Bejan, Tree-shaped insulated designs for the uniform distribution of hot water over an area, Int. J. Heat Mass Transfer 44 (2001) 3111–3123.
[17] W. Wechsatol, S. Lorente, A. Bejan, Development of tree-shaped flows by adding new users to existing networks of hot water pipes, Int. J. Heat Mass Transfer 45 (2002) 723–733.
[18] W. Wechsatol, S. Lorente, A. Bejan, Optimal tree-shaped networks for fluid flow in a disc-shaped body, Int. J. Heat Mass Transfer 45 (2002) 4911–4924.
[19] W. Wechsatol, S. Lorente, A. Bejan, Dendritic heat convection on a disc, Int. J. Heat Mass Transfer 46 (2003) 4381–4391.
[20] A. Bejan, Dendritic constructal heat exchanger with small-scale crossflows and larger-scales counterflows, Int. J. Heat Mass Transfer 45 (2002) 4607–4620.
[21] A.K. da Silva, S. Lorente, A. Bejan, Constructal multi-scale tree-shaped heat exchanger, J. Appl. Phys. 96 (2004) 1709–1718.